STATIC STRUCTURAL ANALYSIS OF S-LAY PIPE LAYING WITH A TENSIONER MODEL BASED ON THE FRICTIONAL CONTACT

S. Ivić[1*] – M. Čanađija[1] – S. Družeta[1]

[1]Faculty of Engineering, University of Rijeka, Faculty of Engineering, Vukovarska 58, 51000 Rijeka

ARTICLE INFO

***Article history*:**
Received: 18.09.2013.
Received in revised form: 21.03.2014.
Accepted: 24.03.2014.

Keywords:
Pipe laying
S-lay
Abaqus
Geometric nonlinearity
Contacts
Friction

Abstract:

Static structural analysis of a pipe during laying is usually performed by use of finite element analysis tools specialized for this purpose. In this paper, Abaqus/CAE, which is general purpose FEA software, was used for a static non-linear structural analysis of a pipe during pipe laying. The pipe is modeled as a geometrically non-linear elastic beam supported by a vessel and its stinger in the overbend region and by the seabed in the sagbend region. We propose a new method for tensioner modeling based on friction contacts between the pipe and the tensioner. Contact interactions between the pipe and rollers, as well as between the pipe and the seabed, are also considered. Basic static analysis is enhanced with floating stinger implementation, a non-flat seabed profile and buoyancy tanks application. The model results for various test cases of pipe laying are compared with an industry standard pipe laying modeling tool.

1 Introduction

The S-lay method of pipe laying has the widest field of action: it can be applied to almost all sizes of pipelines in water depths from shallow to very deep. Because of these characteristics, it is the most commonly used method for laying sub-sea pipelines. When performing S-lay pipeline installation, the pipe is eased off the stern of the vessel while being held by the tensioner mechanism and supported by rollers on the vessel, Fig. 1. Usually, there is an extension attached to the vessel, called the stinger, which provides additional rollers to support the pipe. The weight of the pipe curves the pipe downward until it has reached the seabed. Depending on the curvature of the elastic line of the deformed pipe, the pipe is divided in two regions: an overbend region for concave and a sagbend region for convex geometry of the deformed pipe. A finite element analysis of the pipe during pipe laying has been widely used in industry and science for decades. The elastic model of the pipe during pipe laying is distinctly nonlinear. Two types of nonlinearities appear in the model: geometric nonlinearity and contact interactions.

The most significant influence of geometric nonlinearity regarding modeling of tensioner is manifested through shortening of the horizontal distance of the pipe start or end point, due to deformation of the pipe caused by its own weight.

* Corresponding author.
E-mail address: stefan.ivic@riteh.hr

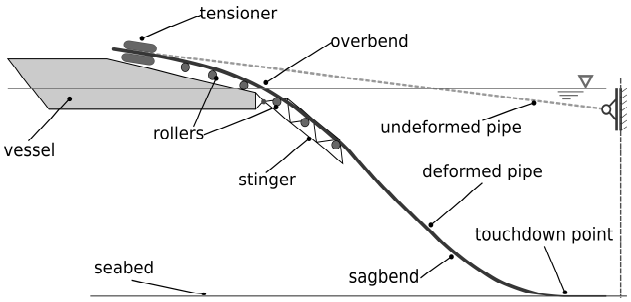

Figure 1. Basic model sketch and nomenclature of S-lay pipe laying method.

The axial force in the pipe exerted by the tensioner cannot be achieved with a simple *a priori* defined axial load on the pipe start node, because in that case the pipe end point should be fixed and the deformed pipe start point, in general, is not positioned at the tensioner exit. There are several approaches to accomplishing the needed axial force in the pipe at the tensioner exit.

Most commonly, the tensioner is modeled as a linear spring element which connects a barge and a pipe [1-4]. The spring is acting along the axis of the pipe and the desired axial force is gained by varying the stiffness of the spring. The lateral movement in the tensioner is prevented with two contact surfaces, one on each side of the pipe. A nonlinear spring can also be used, but it is more suitable for dynamical analysis [1, 5-6]. The stiffness of the spring cannot be determined in advance due to the influence of pipe properties, barge and stinger supports position and water depth on the shape of the deformed pipe and consequently on the position of the pipe start point. Variation of spring stiffness is usually done within an external iterational procedure or it is built in an iterative nonlinear FEM solver.

Another technique for attaining tensioner force uses the varying axial force at the end of the pipe [7-8]. The start of the pipe is pinned to the tensioner and its end is free. The axial force in the pipe is reduced along the pipe due to support reaction forces and the applied load at the end of the pipe is unknown. Adapting the magnitude of the applied load produces a desired axial force at the start of the pipe.

For the research presented in this paper, Abaqus/CAE Student Edition [9] is used to model elastic behavior of the pipe and its interaction with the vessel, the stinger and the seabed. The tensioner interaction with the pipe is modeled as a frictional contact, which is a new approach to pipe laying modeling. In the first part of this paper, a basic model of pipe laying is presented. In the second part, for the purpose of observing tensioner model behavior in specific conditions, the basic model is extended with a floating stinger, buoyancy tanks and non-flat seabed profile implementation. Results for different test cases are presented and compared with the results of industry standard pipe laying modeling tool OFFPIPE.

2 Modeling basic S-lay

To provide an accurate model for pipe laying, all physical phenomena of laying should be taken into account.

The static analysis is conducted in several simulation phases, as described below, with geometric nonlinearity enabled, in which different loads and boundary conditions are gradually introduced.

2.1 Deformable and rigid structures

The barge coordinate system, referred to the sea level and the tensioner exit point, was taken as a principal coordinate system for the analysis. Additionally, the stinger coordinate system is used to define the geometry of the stinger structure. The origin of a stinger coordinate system is positioned on the hinge node of the vessel and the rotation of the stinger coordinate system is defined by the stinger angle Fig. 2.

The vessel and stinger structures are not subjected to deformation and they are defined as rigid bodies. The geometry of the vessel and the stinger is simplified and their dimensions are defined in Table 1. The stinger angle, for the basic S-lay analysis case, is 22°.

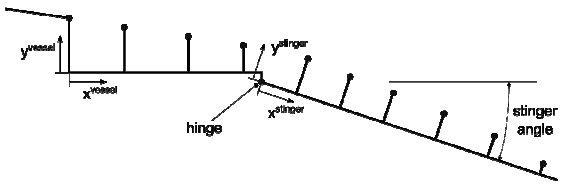

Figure 2. Simplified geometry of vessel and stinger with defined associated coordinates systems.

In the basic analysis case, the sea bottom is assumed to be horizontal and flat at the depth of 80 m. The

seabed profile is also regarded as rigid. All rigid structures (vessel, stinger and seabed) are meshed with R2D2 discrete rigid elements: a 2-node 2D linear rigid link [10]. The vessel and the stinger are meshed with one element per line (see Fig. 2), and the seabed is meshed with 40 elements.
The pipe is modeled as a Timoshenko beam using B21 beam element available in *Abaqus Standard* [10]. The B21 beam element uses a linear shape interpolation function; it allows transverse shear behavior which implies that the cross-section does not necessarily remain normal to the beam axis, and it is well suited for beam models involving contacts. The pipe is 430 m long and angled coincidentally to the tensioner slope. The axial position of the pipe is defined relatively to the tensioner exit node, Table 1, in a way that a 400 m long section of the pipe is positioned right to the tensioner exit node and remaining 30 m long section rests on the left side of the tensioner. The pipe is uniformly meshed with the element length of 1 m, producing 430 elements overall.

Table 1. Vessel and stinger geometry.

Vessel	x [m]	y [m]
Tensioner	0.0	5.80
Vessel roller 1	11.0	4.79
Vessel roller 2	22.0	3.33
Vessel roller 3	33.0	1.22
Vessel hinge	36.0	-2.0
Stinger	x [m]	y [m]
Stinger hinge	0.0	0.00
Stinger roller 1	8.0	3.17
Stinger roller 2	19.0	3.86
Stinger roller 3	30.0	3.92
Stinger roller 4	41.0	3.44
Stinger roller 5	52	2.40
Stinger roller 6	62	1.20
Stinger tip	65	0.00

The pipe used as a test case is a 14 in bare steel pipe. Pipe geometry and material properties are given in Table 2.

2.2 Boundary conditions

The change of the vessel's draft and trim is negligible due to considerably greater mass of the vessel compared to the weight of pipe. Thus, translational movement and rotation of the vessel

Table 2. Pipe properties.

Property	Value
Young's modulus	207 GPa
Poisson's ratio	0.3
Pipe outside diameter	355.6 mm
Pipe wall thickness	20 mm
Pipe length	430 m

structure is prevented. In reality, horizontal displacement of the vessel is detained by anchors. Based on the given assumptions, boundary conditions for the vessel structure are:

$$u_x^{vessel} = 0, \quad u_y^{vessel} = 0, \quad \varphi^{vessel} = 0 \qquad (1)$$

where u_x is horizontal displacement, u_y is vertical displacement and φ is angular displacement. In the basic static analysis, the stinger structure if fixed to the vessel on a hinge and together they form an unmovable and undeformable structure. Displacement boundary conditions of the stinger are applied to a hinge node:

$$u_x^{stinger} = 0, \quad u_y^{stinger} = 0, \quad \varphi^{stinger} = 0. \qquad (2)$$

The pipe slips through the tensioner grip, therefore the pipe must be extended beyond the tensioner to avoid dropping from the vessel. The extended part of the pipe is consistently supported by the lower part of the tensioner to avoid unnecessary/unwanted pipe bending.
The ending node of the pipe is fixed to the virtual vertical guideline that represents the connection of the analyzed part of the pipe to the remaining pipe that has been already laid on the seabed. Boundary conditions applied to the pipe ending node prevent its horizontal displacement:

$$u_x^{end} = 0. \qquad (3)$$

2.3 Loads

The pipe is directly subjected to two principal loads: pipe weight and pipe buoyancy, and additionally to forces produced in contacts with the tensioner, the rollers and the seabed.
The pipe weight per length is calculated according to material density and cross section dimensions:

$$w_P = \frac{(D^2 - (D - 2 \cdot s)^2) \cdot \pi}{4} \cdot \rho_P \cdot g \qquad (4)$$

where D is the pipe outside diameter, s is the pipe wall thickness, ρ_P is the density of pipe material and g is a gravitational constant. The pipe weight for the parameters given in Table 2 and the density ρ_P=7850 kg/m^3 is w_P=1623.3 N/m.

Regarding pipe buoyancy, two parts of the pipe must be considered separately: the unsubmerged part of the pipe and the submerged one. Only the submerged part of the pipe is subjected to buoyancy. The pipe buoyancy per length is:

$$w_B = \frac{D^2 \cdot \pi}{4} \cdot \rho_W \cdot g \qquad (5)$$

where ρ_W is water density. For water density ρ_W =1025 kg/m^3, pipe buoyancy per length is w_B=998.3 N/m.

Because of inability to *a priori* determine the boundary between the unsubmerged and the submerged part of the pipe, the pipe weight is introduced in two simulation phases (phase 2 and phase 3). In the second phase, the pipe weight reduced by pipe buoyancy is applied to the whole pipe. In the third phase, after obtaining deformed pipe geometry from the second phase, additional weight is applied only to the unsubmerged part of the pipe ($y > 0$).

Based on the weight of the pipe and its buoyancy, the line load is calculated:

$$q_y^{pipe} = -w_P + w_B = -625 \text{ N/m} \qquad (6)$$

and it is applied to the whole pipe. The additional line load is applied to the unsubmerged part of the pipe in the third phase of the analysis

$$q_y^{unsubmerged} = -w_B = -998 \text{ N/m} \qquad (7)$$

which results in the total load of 1623 N/m on the unsubmerged part of pipe. Beside previously mentioned external loads, the tensioner grip force is also applied to the pipe, albeit indirectly. The tensioner grip force is a product of frictional contact, and therefore it is explained in the Contacts subsection.

2.4 Contacts

The contact problem is present in the pipe interaction with the tensioner, vessel rollers, stinger rollers and in the pipe interaction with the seabed. The tensioner is modeled as a pair of surface-to-surface finite sliding contacts. The lower part of the tensioner is a 1D rigid structure attached to the barge. The upper part of the tensioner is also a 1D rigid body which moves perpendicularly to the tensioner axis, Fig. 3.

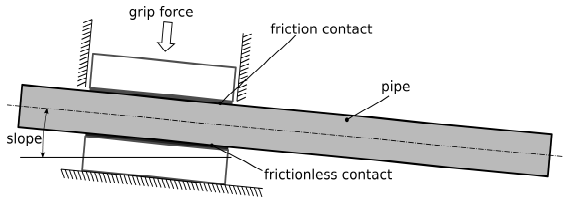

Figure 3. Schematic representation of frictional contact in tensioner.

The tension force exerted on a pipe appears as a counter force to the hung pipeline weight. It is enacted by tensioner grip force through a friction contact between the tensioner and the pipe. The basic friction model, based on Coulomb's friction law, is used to turn the grip force into the tension force:

$$T = \mu \cdot F_G \qquad (8)$$

where T is the tension force, F_G is the grip force and μ is the static friction coefficient. The grip force F_G is applied to the upper part of the tensioner, perpendicularly to the tensioner axis. For convenience, the friction coefficient is set to 1 in order to produce the tension force equal to the applied grip force. It should be noted that achieved tension force can be less than aimed if the applied grip force is excessive for the given pipe weight. The presented model of the tensioner, although not representing real tensioner mechanics and behavior, takes into account all the influences of the tensioner on pipe: the pipe is gripped in the tensioner and the tension force is uniformly applied to the pipe along the tensioner contact. Normal behavior of both tensioner contacts is linear pressure over-closure with contact stiffness equal to 50 MN/m.

In all pipe laying test cases, the tensioner force T=245.17 kN (equivalent to 25 metric tons) is

reached with an applied tensioner grip force of the same magnitude. The tension force is small enough and it can always be achieved with given pipe properties, water depth and pipe length. Tensioner slope $\alpha = 4.65°$ is used. Frictional contact is established along the tensioner contact surface, which is 5 m long.

The contact between the pipe and a roller is established in a single point because of geometrical representation of the roller. The pipe-roller contact is modeled as a contact with finite-sliding tracking and node-to-surface contact discretization. Unlike pipe-roller contacts, the contact between the pipe and the seabed is established along the curve of the seabed and it is modeled as finite-sliding tracking contact with surface-to-surface discretization approach. Behavior of the pipe in the contact with the seabed is explained in detail in [11-12].

For all contacts, only the normal reaction of the contacts was considered, with linear pressure over-closure and with contact stiffness equal to 50 MN/m for pipe-roller contact and 40 MN/m for pipe-seabed contact.

2.5 Analysis options

Abaqus Standard General Static analysis is conducted in several phases, in which loads, boundary conditions and contacts can be enabled, disabled or modified. Each loading phase of the analysis is accomplished with incremental load introduction.

An incremental procedure automatically varies load increments on the basis of geometric nonlinearity which includes large deformation and contact establishment. Abaqus analysis increments can be interpreted as time in quasi dynamic analysis in which loads are gradually introduced over time. The terms "increment size" and "load introduction progress" are adopted to define the portion of loads introduced in each increment and cumulative portion of calculated phases, respectively.

The basic pipe laying analysis is performed in three general static phases, Table 3, which differ only in application of loads and phase incrementation parameters. Geometric non-linearity is enabled in all three phases. The model is solved through automatic incrementation of loadings introduced in each phase. Parameters of automatic incrementation are given in Table 3. In the first phase, only tensioner grip force is applied, and a pipe contact with a lower and upper part of the tensioner is established. Pipe submerged weight producing deformation of the pipe is introduced in the second phase. During the second simulation phase contacts of the pipe with rollers and the seabed are established. In the third phase, based on the deformed pipe, additional weight is applied to the part of the pipe above the sea level.

If it turns out that the difference of the pipe start node displacement, after applying additional weight, is significant, the introduction of additional unsubmerged pipe weight should be conducted in two or more simulation phases. In analysis phases, additional pipe weight should be progressively introduced in a way that the total additional pipe weight is applied to the last simulation phase. In the preceding phases, the partial additional pipe weight is applied to the unsubmerged part of the pipe. Although the analysis is to be based on the results obtained in the final phase, intermediate phase results are very useful for understanding the proposed model for pipe laying.

Table 3. Abaqus analysis procedure.

	Phase 1	Phase 2	Phase 3
Grip force	Introduced		
Submerged pipe weight		Introduced	
Pipe in air weight			Introduced
Maximum number of increments	10	1000	100
Initial increment size	1	10^{-4}	1
Minimum increment size	0.1	10^{-5}	0.01
Maximum increment size	1	0.1	1

3 Advanced S-lay features

3.1 Floating stinger

The floating stinger is a stinger that can rotate about the hinge while additionally being supported by its own buoyancy. The stinger position (angle of the stinger) depends on rollers reaction forces; hence it cannot be determined before the analysis has been conducted. The floating stinger model allows for the stinger to rotate around the hinge and the resultant force of the weight of the stinger structure, stinger buoyancy and weight of ballast water is applied to the stinger structure, Fig. 4. The stinger will attain the position (angle) where equilibrium of the resultant force and rollers reactions is achieved. Since the stinger can rotate and the upthrust force is always vertical and acting on the same position on the stinger, the torque produced in this way varies depending on the angle of the stinger.
Boundary conditions for the floating stinger are applied to a stingers hinge node:

$$u_x^{stinger} = 0, \quad u_y^{stinger} = 0 . \tag{9}$$

Boundary condition for the floating stinger Eq. (9), as opposed to fixed stinger boundary condition Eq. (2), allows rotation about the hinge.

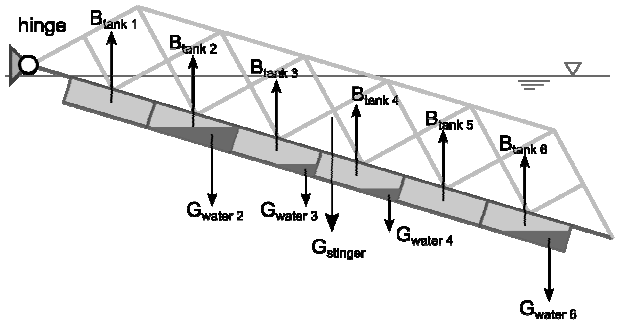

Figure 4.Floating stinger known forces components.

For the floating stinger test case, an additional simulation phase is introduced after the second phase in which stinger rotation is allowed and total upthrust force is appointed to the stinger, Fig. 4. The fourth phase of the floating stinger analysis test case is the same as the third phase of the basic analysis test case in which additional weight is applied to the unsubmerged part of the pipe. The upthrust force of 115 kN acting on a 44.65 m long lever arm produces the maximal torque (in a horizontal position of the stinger) of 5135 kNm about the hinge.
It should be noted that the initial stinger angle (which is fixed in the first two phases) should not be greater than the final angle of the floating stinger since the pipeline cannot be pushed backward through tensioner due to already established full frictional force in the pipe-tensioner contact. At the same time, the initial stinger angle should be close enough to the final floating angle so as to avoid redundant analysis incrementation. For this test case, the initial stinger angle is 22°.

3.2 Non-flat seabed

Structural analysis of pipeline laying on the non-flat seabed requires changes of seabed geometry. The non-flat seabed is most easily defined using multiple connected lines forming a polyline. For the analysis with the non-flat seabed, a new test case is made based on the basic analysis model with the changed seabed profile, Table 4, Fig. 5. The seabed profile used in this case is designed to provide multiple separate sections of the pipe-seabed contact. The mesh of the seabed structure is generated on a seed of one element per polyline segment with one dimensional R2D2 discrete rigid element.
Extending the basic model geometry with the rough seabed allows for detailed observations of stress and strain on the pipe which is laid on the seabed. Unlike the basic model, the contact between the pipe and the bottom is not continuous, and it is possible to observe free spans (unsupported parts of the pipeline extending above the “valleys” on the sea bottom). Due to an intermittent contact of the pipelines and the non-flat sea bottom, pipe bending occurs even after reaching the touch-down point.

3.3 Buoyancy tanks

Buoyancy tanks are installed on heavy pipes to prevent excessive stress and deformation of the pipe. They are installed on a pipe on a vessel and they are, usually, uniformly distributed along the pipeline and removed after reaching the touchdown point on the sea bottom.
Buoyant tanks are modeled as vertical concentrated forces acting directly on the pipe. Since the pipe used in the primary analysis would be too light to

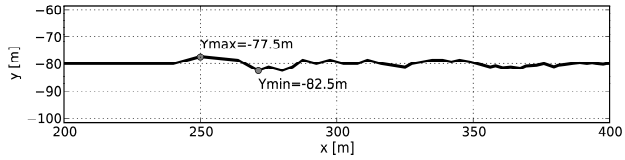

Figure 5. Non-flat seabed profile.

Table 4. Coordinates of seabed points.

x [m]	y [m]	x [m]	y [m]	x [m]	y [m]
200.00	-80.00	283.75	-81.25	358.18	-80.81
205.00	-80.00	287.50	-78.75	360.84	-81.51
210.00	-80.00	292.50	-80.00	363.75	-81.25
215.00	-80.00	297.50	-78.75	367.25	-81.71
220.00	-80.00	302.50	-80.00	369.33	-80.88
225.00	-80.00	307.50	-80.00	373.21	-80.63
230.00	-80.00	311.25	-78.75	375.92	-80.05
235.00	-80.00	316.25	-80.00	379.59	-81.18
240.00	-80.00	320.62	-80.62	381.27	-80.61
245.00	-78.75	325.00	-81.25	383.53	-80.37
250.00	-77.50	327.50	-80.00	386.65	-79.97
254.58	-77.92	331.25	-79.38	389.10	-79.73
259.17	-78.33	335.00	-78.75	391.69	-80.02
263.75	-78.75	338.75	-78.75	393.59	-79.79
267.50	-80.62	341.98	-79.38	395.00	-80.00
271.25	-82.50	345.00	-78.75	397.63	-80.25
275.00	-81.25	349.08	-79.43	398.95	-80.01
280.00	-82.50	356.25	-81.25	400.00	-80.00

Table 5. Pipe properties for buoyancy tanks test case.

Property	Value
Pipe outside diameter	254 mm
Pipe wall thickness	24 mm
Submerged pipe weight	825.7 N/m
Unsubmerged pipe weight	1335 N/m

apply buoyancy tanks, the pipe with heavier submerged weight is used for analysis with buoyancy tanks, Table 5. Properties that are not listed in Table 5 are the same as in the basic test case. In the buoyancy tanks test case, the distance between the buoyancy tanks is 48 m (the length of two pipe joints) and buoyancy of each tank is equal to 21.575 kN (equivalent to 2.2 metric tons).

4 Results

Results presented in this paper contain only quantities interesting from offshore engineering perspective [13-17]. Offshore standards propose design criteria based upon bending moment, axial forces and strain. Since the presented analysis cases are based on the linear material and an invariable pipe cross-section over the pipe length, the strain is proportional to the bending moment and thus only the bending moment is presented in the results. The nomenclature used in the result figures is: BM for the bending moment, *Q* for the shear force and N for the axial force. Although only the results of the final simulation phases when all loads are applied are relevant, some intermediate phases are shown to interpret interesting effects that happen during analysis convergence.

4.1 Basic model results

Abaqus solved general static phases using automatic incrementing introduction of loads. The solution of the basic pipe laying model was completed after the total of 49 increments in which all external loads were applied, Fig. 6.

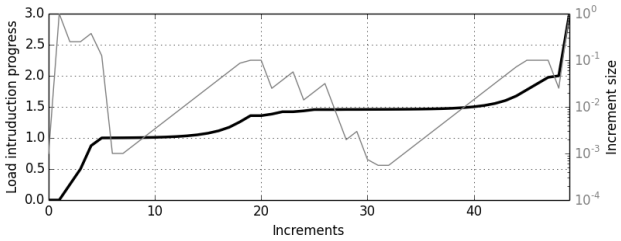

Figure 6. Load introduction incrementation.

Most of conducted increments are needed for solving the second simulation phase in which the pipe is subjected to its weight, causing large displacements and severe geometric nonlinearity. Furthermore, contacts with the rollers and the seabed are established in the second simulation phase, which causes variation of the load introduction increment size.

The pipe deformed under the load of its own weight forms a typical “S” curve, Fig. 7. The pipe pulled by its own weight through tensioner frictional contact has displacement along the tensioner axis of the first node of the pipe of 14.87 m in the second phase and 15.41 m in the third phase. There is no need for additional phases as there are no significant changes

in the geometry after the second phase, at least not in the region where additional weight of the pipe is applied. If displacement of the pipe has significantly changed after the phase including additional weight of the unsubmerged pipe, then the introduction of additional weight should be performed in multiple phases (as it was done in the test case with buoyancy tanks applied to the pipe).

Regarding the deformed pipe geometry, the slope of the pipe can also be observed, Fig. 8. It is visible that the inflection point of the deformed pipe "S" curve is located approximately at the minimum of the slope curve. Bending moment is the most used criteria for the pipe installation in offshore industry [18]. The bending moment and shear forces, Fig. 9 and Fig. 10, are influenced by rollers reaction forces, which are manifested in peaks in both diagrams. Notice the positive sign of the bending moment in the overbend region and the negative sign in the sagbend region. The sign of bending moment changes at inflection point noted in the slope plot, Fig. 8. Unlike geometry and displacement, the bending moment and shear forces have significantly changed in the second phase in a region when pipe buoyancy has changed.

The axial force is the basic result needed for calculating Effective Axial Force criteria for submarine pipelines [17]. Friction force is uniformly applied to the pipe along the tensioner contact length in order to provide the tension force. The axial forces plot, Fig. 11, shows that the axial force right at the tensioner exit amounts to 243.16 kN, which is practically equal to the aimed tension force, thus

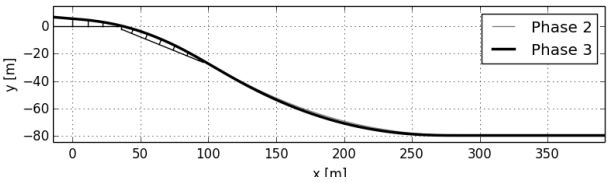

Figure 7. Deformed pipe geometry.

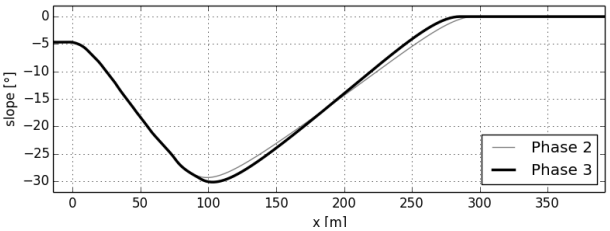

Figure 8. Pipe slope.

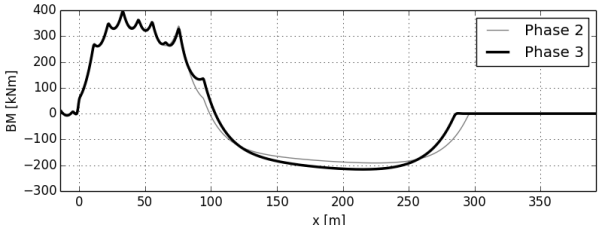

Figure 9. Bending moment diagram.

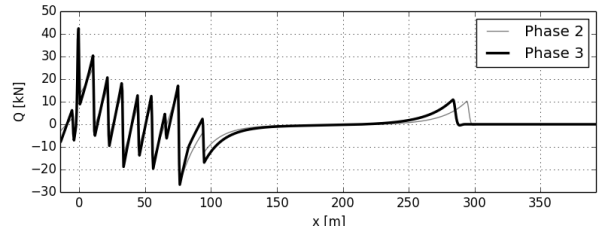

Figure 10. Shear forces diagram.

proving that the tensioner contact model works as presumed. The small negligible difference between the axial force on the tensioner exit and the tension force (245.17 kN) is caused by the weight of the part of the pipe that did not enter the tensioner. Since there are no shear contact forces of rollers, the axial force is influenced only by tensioner friction force and pipe weight. Due to uniformly distributed pipe weight, axial forces plotted as a curve smoothly follows the tensioner contact. The axial force in the pipe laid on the seabed is important for other analyses such as the free span analysis.

4.2 Floating stinger test case results

The most important characteristic of pipe laying analysis with the floating stinger is the establishment of the stinger position which satisfies static equilibrium, Fig. 12. After allowing rotation of the stinger and introducing the stinger upthrust force in the third phase of the analysis, the stinger rigid structure has been positioned based on its upthrust force and rollers reactions. The additional pipe weight, applied in the fourth phase, also greatly influences the stinger load balance and its final position. The achieved stinger angle is 18.28° and 21.26° in the third and fourth phase, respectively. The first pipe node displacement is observed to have determined the length of pipe sliding due to the stinger angle change. The pipe slid through tensioner and achieved displacement of 14.93 m,

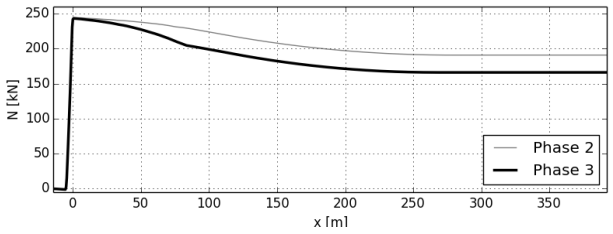

Figure 11. Axial forces diagram.

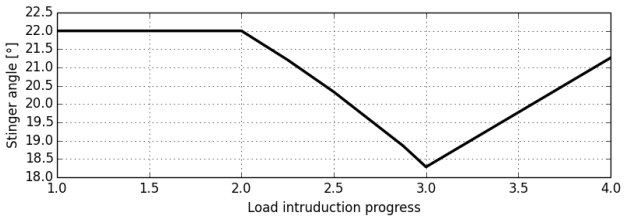

Figure 12. Angle of stinger over load introduction increments.

14.93 m and 15.33 m in the second, third and fourth simulation phase, respectively. In the third phase, in which stinger rotation was allowed, the pipe did not slide through the tensioner in either direction because the tension force was not surpassed due to raising of the stinger. Structural analysis results obtained from the floating stinger test case after each simulation phase can be compared, Fig. 13. All differences in the results shown in Fig. 13 are predominantly influenced by the stinger angle and the application of the unsubmerged pipe weight which are introduced in the third and fourth simulation phase. Consequently, different roller contacts have been established, yielding significant differences in results, especially in the bending moment and shear forces.

The produced tensioner force, observable as the pipe axial force at the tensioner exit, should be compared with the value of reached tension after the final phase of the floating stinger analysis. The axial force at the tensioner exit in the third simulation phase is lower than expected. This is caused by rising the stinger, which diminished the tension in the pipe achieved by the frictional contact in the tensioner. Although the result of the third phase is not valid by itself, it is legit within the whole analysis as the effect of diminished tension is completely neutralized by the effect of the additional unsubmerged pipe weight in the fourth simulation phase.

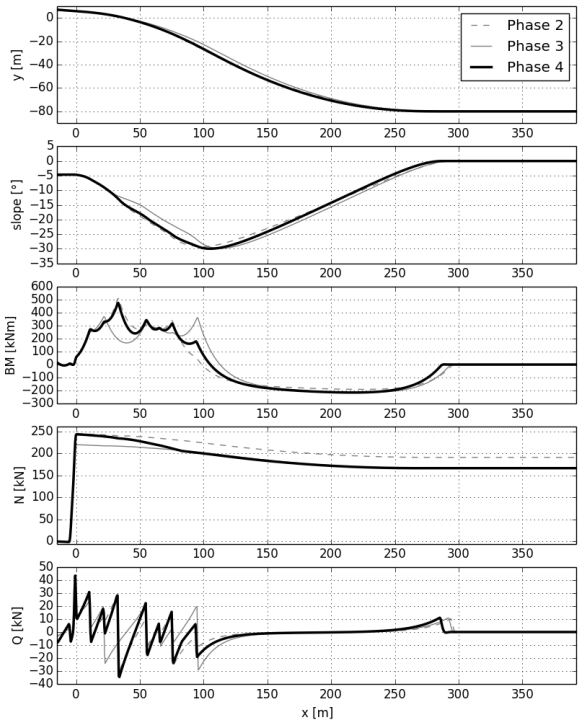

Figure 13. Results of floating stinger test case.

4.3 Non-flat seabed test case results

The structural analysis of a pipe during installation on non-flat seabed provides useful information on pipe interaction with the seabed, Fig. 14. Moderately non-flat seabed mostly impacts the sagbend region of the pipe and the part of the pipe that is laid and in contact with the seabed. The non-flat seabed has greater influence on the overbend region of the pipe due to highly variable sea bottom depth and highly variable pipe slope at the touchdown point. As in the analysis of the basic test case, displacement of the pipe after introducing additional weight onto the unsubmerged part of the pipe has not significantly changed (14.59 m after third simulation phase and 14.93 m after the fourth simulation phase) and therefore there is no need for introducing additional pipe weight to the unsubmerged part of the pipe. The non-uniformly supported pipe, due to the rough seabed, produces peaks in shear forces and consequentially in bending moment. The deformed pipe is forming free spans – segments of the pipe laid on the seabed between two seabed peaks. Since the contact of the pipe and the seabed has been modeled as a contact without friction, there is no impact of the seabed profile on the axial force.

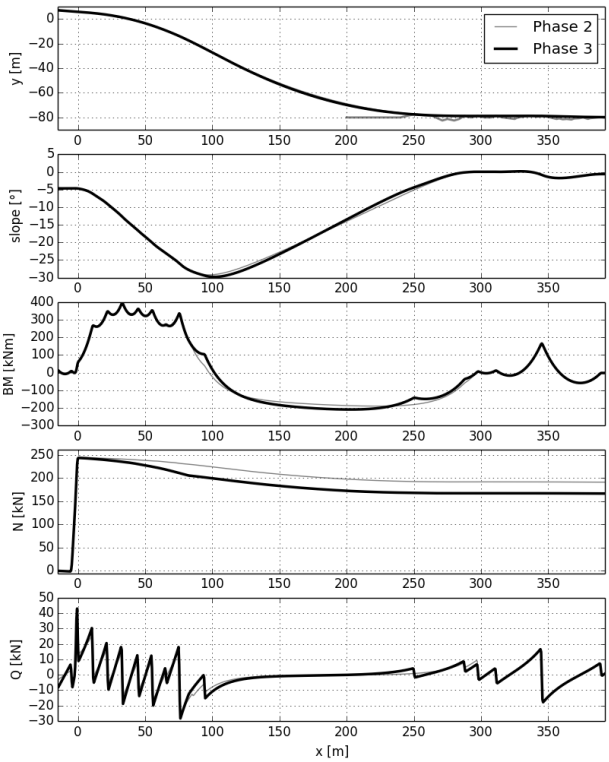

Figure 14. Results of non-flat seabed test case.

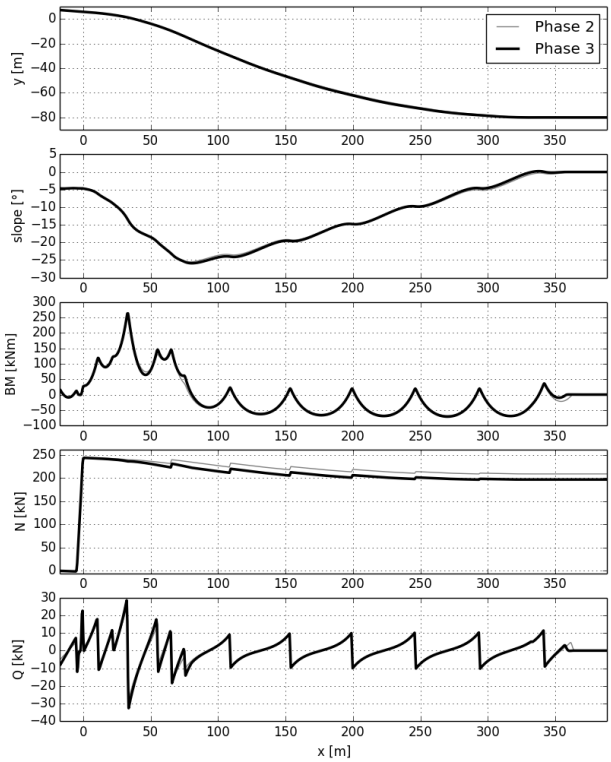

Figure 15. Results of buoyancy tanks test case.

4.4 Buoyancy tanks test case results

In the analysis with buoyancy tanks applied to the pipe, pipe starting node displacement is 12.26 m and 12.55 m for the second and third simulation phase, respectively. Buoyancy tanks implementation greatly determines the outcome of pipe laying structural analysis Fig. 15. Since buoyancy tanks are modeled as concentrated forces acting on a pipe, they produce local effects manifested as jumps in all observed results. Seven buoyancy tanks are applied to the pipe, of which six are positioned after the last roller of the stinger.

Because of the vertical action of buoyancy tank forces, the influence of buoyancy tanks on the pipe axial force can be noted, especially in the region with a sharper pipe slope.

5 Tensioner model validation

Pipe laying analysis with a frictional contact tensioner model performed on the pipe laying case is shown in [19]. It is a two dimensional static pipe laying analysis case using a fixed stinger.

The geometry of a barge is defined using a constant radius of the curvature: the heights of the supports are set on an arc of a circle. The circle arc is tangent to the tensioner at the tensioner exit node located at 24.442 m above the sea level with 0.6° tensioner slope. Following the tensioner, five supports are equally spaced at stern with a spacing of 12.192 m (40 ft) along the stern. The elevations of the supports are defined so as to allow for the supports to be positioned at the radius of 219.456 m (720 ft). The stinger geometry is also defined using the radius of curvature and tangency. Stinger circle arc is tangent to the barge circle arc and its radius is 195.072 m (640 ft). The pipe supports on a stinger are placed 9.144 m (30 ft) apart.

The pipe used in this case is a 16 in pipe (outside diameter is 0.406 m) with the wall thickness of 1.27 cm. Elastic modulus of pipe material is 196.5 GPa. The line load representing submerged pipe weight is 1359 N/m, and an additional load of 2092.26 N/m for the unsubmerged part of the pipe. The tensioner force of 444.8 kN has been achieved by the tensioner friction contact over the length of 25 m. The seabed is flat at the depth of 91.44 m. The results for the described pipe laying analysis case are obtained with OFFPIPE [19]. OFFPIPE is one of the leading software solutions for finite element analysis of pipe laying and is commonly

used in offshore industry, thus being a good candidate for pipe laying model validation and comparison. In OFFPIPE, the tensioner has been modeled as a spring element [1] which is an essentially different approach from the one presented in this paper.

The described pipe laying case has been modeled in Abaqus with the use of techniques presented in this paper and the obtained results are compared with the results given in [19].

As it can be seen in Fig. 16, the results obtained from the model with a frictional contact tensioner made in Abaqus almost perfectly match OFFPIPE results. It is obvious that the same beam model is used in both cases. The difference in the compared models is the method used to achieve the axial force at the start of the pipe. Based on the effective axial force plotted in Fig. 16, it can be concluded that the tensioner model based on a frictional contact can provide the same purpose using a completely different approach to tensioner modeling.

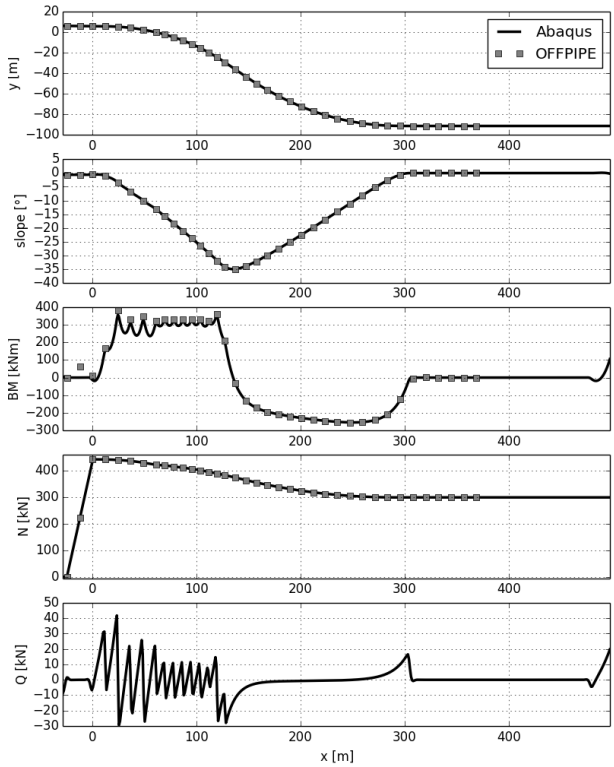

Figure 16. Comparison of Abaqus and OFFPIPE results.

6 Conclusion

The presented procedure for the static structural analysis of S-lay pipeline installation introduces tensioner modeling as a frictional contact using Abaqus Standard, a general purpose finite element analysis tool. The analysis of various test cases, covering a basic S-lay model, the floating stinger, the non-flat seabed and laying with buoyancy tanks, confirms adequacy and accuracy of the proposed tensioner model. Moreover, the results obtained with the tensioner model based on frictional contact match closely the results obtained by leading software used in offshore industry. The test cases used in the paper successfully reproduce various behaviors and effects of the given model in specific conditions.

The proposed frictional model of a tensioner gives some advantages in comparison to the commonly used models. Since a typical pipe laying process uses multiple tensioners, the possibility to extend the pipe laying model with additional tensioners may be very useful. The presented pipe laying model with the proposed tensioner model allows for the easy implementation of multiple tensioners, which enables a detailed analysis of pipe behavior in the tensioner system. Furthermore, the model can incorporate a more realistic geometrical representation of the tensioner and possibly a deformable tensioner structure, which enables the structural analysis of the tensioning system. The proposed model could be easily extended so as to allow for the analysis of pipe laying with the variable cross section and material properties along the pipeline, or for the analysis of pipe and cable combinations to simulate offshore operations such as shore-pull or abandonment-and-recovery. Eventually, the analysis with the deformable stinger would give an insight into structural and elastic behavior of the stinger structure. The frictional tensioner model, or at least its basic principle, could also be used in the dynamical structural analysis of pipe laying.

References

[1] Malahy Jr R.: *Nonlinear finite element method for the analysis of the off-shore pipe laying problem*, Ph.D. thesis, Rice Univ., Houston, 1985.

[2] Hvidsten E.: *Pipe laying on uneven seabed*, Master's thesis, University of Stavanger, 2009.

[3] Hong W.: *Simulation of TDP Dynamics during S-laying of Subsea Pipelines*, Master thesis, Norwegian University of Science and Technology, 2010.

[4] Langhelle M. B.: *Pipelines for Development at Deep Water Fields*, master thesis, University of Stavanger, 2011.

[5] Lawinscky da Silva D. M., de Lima M. H. A., Jacob B. P.: *Numerical Model for the Simulation of the Pipeline-Laybarge interaction in pipe laying procedures*, International journal of Modeling and Simulation for the Petroleum Industry 3(2009), 1.

[6] Gaggiotti, F.: *Deep water pipe laying: from mooring-based station keeping to dynamic positioning*, Ph. D. thesis, Universita politecnica delle Marche, 2011.

[7] Yun H. D., Peek R. R., Paslay P. R. and Kopp F. F.: *Loading History Effects for Deep-Water S-Lay of Pipelines*, Journal of Offshore Mechanics and Arctic Engineering, 126(2), 156-163, 2004.

[8] Sun J., Jukes P.: *From Installation To Operation-A Full-Scale Finite Element Modeling Of Deep-Water Pipe-In-Pipe System*, Proceedings of the ASME 28th International Conference on Ocean, Offshore and Arctic Engineering, 2009.

[9] Dassault Systèmes, *Abaqus 6.11 Abaqus/CAE User's Manual*, 2011.

[10] Dassault Systèmes, *Abaqus 6.11 Analysis User's Manual*, 2011.

[11] Randolph M. F., White D. J.: *Pipeline embedment in deep water: processes and quantitative assessment*, in: Proceedings of the 40th Annual Offshore Technology Conference, Houston, 2008.

[12] Leepipatpaiboon W.: *An Aprropriate FEA Modeling Technique for OnBottom Roughness Analysis*, Ph.D. thesis, Asian Institute of Technology, 2010.

[13] Veritas D.N.: *Offshore Standard DNV-OS-F101: Submarine Pipeline Systems*, 2010.

[14] Spinelli C., Demofonti G., Fonzo A., Lucci A., Ferino J., Di Biagio M., Flaxa V., Zimmermann S., Kalwa C., Knoop F.: *Full Scale Investigation on Strain Capacity of High Grade Large Diameter Pipes*, 2011.

[15] Torselletti E., Asa S., Mørk K.J.: *Submarine Pipeline Installation JIP: Strength and Deformation Capacity of Pipes*, International Conference on Offshore Mechanics and Arctic Engineering, 2006.

[16] Braskoro S., Dronkers T., Van Driel M.: *From Shallow to Deep Implications for Offshore Pipeline Design*, Journal of The Indonesian Oil and Gas Community, Komunitas Migas Indonesia, 2004.

[17] Fyrileiv O., Collberg L.: *Influence of pressure in pipeline design–effective axial force*, 24th International Conference on Offshore Mechanics and Arctic Engineering, 2005.

[18] Hauch S., Bai Y.: *Bending moment capacity of groove corroded pipes*, ISOPE-2000, 2000.

[19] Malahy Jr R., *OFFPIPE user's guide*, Version 2.05, Houston, 1996.